Accurate determination of one-bond heteronuclear coupling constants with "pure shift" broadband proton-decoupled CLIP/CLAP-HSQC experiments

István Timári[1], Lukas Kaltschnee[2], Andreas Kolmer[2], Ralph W. Adams[3], Mathias Nilsson[3,4], Christina M. Thiele[2], Gareth A. Morris[3], Katalin E. Kövér[1*]

[1]Department of Inorganic and Analytical Chemistry, University of Debrecen, Egyetem tér 1, H-4032 Debrecen, Hungary

[2]Clemens-Schöpf-Institut für Organische Chemie und Biochemie, Technische Universität Darmstadt, Alarich-Weiss-Straße 4, D-64287 Darmstadt, Germany

[3]School of Chemistry, University of Manchester, Oxford Road, Manchester, M13 9PL, United Kingdom

[4]Department of Food Science, University of Copenhagen, Rolighedsvej 30, DK-1958 Frederiksberg C, Denmark

Abstract: We report broadband proton-decoupled CLIP/CLAP-HSQC experiments for the accurate determination of one-bond heteronuclear couplings and, by extension, for the reliable measurement of small residual dipolar coupling constants. The combination of an isotope-selective BIRD$^{(d)}$ filter module with a non-selective ^{1}H inversion pulse is employed to refocus proton-proton coupling evolution prior to the acquisition of brief chunks of free induction decay that are subsequently assembled to reconstruct the fully-decoupled signal evolution. As a result, the cross-peaks obtained are split only by the heteronuclear one-bond coupling along the F_2 dimension, allowing coupling constants to be extracted by measuring simple frequency differences between singlet maxima. The proton decoupling scheme presented has also been utilized in standard HSQC experiments, resulting in a fully decoupled pure shift correlation map with significantly improved resolution.

Keywords: Broadband proton decoupling; F_2-coupled HSQC; Pure absorption; IPAP; RDC

1. *Introduction*

Residual dipolar couplings (RDCs) provide invaluable long-range constraints for structure determination of molecules, conveying information on the distances between dipolar-coupled nuclei and on the orientations of the corresponding internuclear bond vectors. In recent years residual dipolar couplings have therefore been widely utilized in structural studies of proteins, nucleic acids, carbohydrates, organic and organometallic compounds in the liquid state, and have been shown to improve considerably the precision of structures [1-9].

For weakly aligned samples, RDCs manifest themselves in NMR spectra as an increase or decrease in the splittings due to scalar (*J*) couplings between nuclei. Their magnitudes can therefore be extracted by measuring changes of splitting in isotropic compared to anisotropic sample conditions.

Here we propose a modification of F_2-coupled CLIP/CLAP-HSQC [10] experiments in which the unwanted additional splittings caused by co-evolution of proton-proton couplings are eliminated with the aid of an isotope-selective BIRD-based broadband proton decoupling scheme applied during signal evolution. Thus one-bond heteronuclear couplings can be determined from the resulting spectra simply by measuring the frequency differences between the peak maxima of singlets, instead of between the centers of complex multiplets.

We also demonstrate that the proposed broadband proton decoupling scheme, when built into the standard gradient enhanced HSQC experiment, leads to pure shift correlation spectra of enhanced resolution, offering significant advantages for automated spectral analysis such as automated peak-picking or automated intensity measurement in HSQC-based relaxation experiments.

2. *Experimental*

All experiments were performed on a Bruker Avance II 500 spectrometer (Bruker BioSpin GmbH, Rheinstetten, Germany) equipped with a TXI z-gradient probe. All spectra were processed with TopSpin 2.1, 2.5 or 3.0 (Bruker Biospin GmbH, Karlsruhe, Germany). For testing the experiments a sample of ^{13}C-labeled [C-1]-methyl-α,β-D-glucopyranoside (**1**) (30 mg) dissolved in 500 µl D_2O was used. The measurement of

RDCs was demonstrated on a sample of tetra-sodium-(1-methyl-2,3,4-tri-*O*-sulfonato-6-deoxy-6-*C*-sulfonatomethyl-α-D-glucopyranoside) (**2**) (20 mg), dissolved in 500 µl D_2O for isotropic condition. The liquid crystalline phase was prepared as described by Rückert and Otting [11] from ether/alcohol (hexaethylene glycol monododecyl ether ($C_{12}E_6$)/n-hexanol, 5%, r = 0.64, J_Q = 25 Hz). The $C_{12}E_6$ and n-hexanol were purchased from Sigma–Aldrich and used without further purification. The variants of the HSQC sequence were tested on a sample of D-sucrose (**3**) (30 mg) dissolved in D_2O. For all measurements the nominal temperature was set to 298 K unless indicated otherwise. All F_2-coupled CLIP/CLAP-HSQC spectra were acquired with a high spectral resolution of 0.3 Hz/point, for accurate measurement of small residual dipolar couplings. The ^{15}N-^{1}H pure shift HSQC spectrum was recorded for 1.6 mM [U-^{15}N]-*Penicillium* antifungal protein (PAF) (95% : 5% H_2O:D_2O), pH 5.0, at 300 K.

Spectra were recorded with a proton 90° pulse of 15 µs, a carbon 90° pulse of 15.7 µs for acquisition, a carbon 90° pulse of 80.0 µs for GARP decoupling, smoothed chirp pulses (Crp60,0.5,20.1) of 500 µs duration for broadband ^{13}C inversion and (Crp60comp.4) of 2 ms for broadband ^{13}C refocusing. ^{1}H-^{15}N HSQC spectra were collected with nitrogen 90° pulses of 29 µs for acquistion and 250 µs for WALTZ16 decoupling.

For processing the 3D raw data sets acquired with the pulse sequences presented, a Bruker AU program (available at http://nmr.chemistry.manchester.ac.uk) was used to reconstruct the 2D interferograms. Prior to 2D Fourier transformation, the data were apodized by multiplying with a 90° shifted sine-squared function and then zero-filled by a factor of two in both dimensions, to yield a spectral resolution of 0.3 – 0.5 Hz/point in the ^{1}H dimension.

3. *Results and discussion*

Due to the increasing interest in the use of RDCs in recent years, numerous methods based on measuring frequency differences between multiplet components have been developed for the measurement of one-bond heteronuclear coupling constants. The most widely used approach is based on the HSQC experiment, with heteronuclear couplings retained in the F_1 or F_2 dimension. To circumvent spectral crowding due to the

increased number of cross-peaks in the coupled spectra, E-COSY [12], spin-state selective [13-15], IPAP [16] and TROSY [17-19] methods have been proposed. Unfortunately, all these methods suffer from additional splittings of cross-peaks due to the co-evolution during data acquisition of coupling interactions other than the desired heteronuclear one-bond coupling.

To eliminate line-splittings caused by multiple bond heteronuclear couplings in the F_1-coupled HSQC sequence, a gradient enhanced BIRD$^{(r)}$ module has been employed during the evolution period t_1, yielding simplified cross peaks with only splittings due to the desired one-bond couplings in the F_1 dimension [20, 21]. However, heteronuclear correlation experiments coupled in the indirect F_1 dimension are limited by the necessity of acquiring large numbers of t_1 points to achieve sufficiently high digital resolution, therefore making the experiment rather time-consuming. For this reason, measurement of one-bond heteronuclear coupling constants from F_2 multiplets appears more favorable due to the high digital resolution affordable in the F_2 dimension. However, the complexity and asymmetry of multiplet structures due to proton-proton scalar/dipolar couplings may render the accurate definition of peak positions difficult or even impossible.

A breakthrough in the removal of unwanted line-splittings is offered by the use of broadband homonuclear decoupling methods that have been reported in the last few years [22-31]. Such experiments can be classified into two groups, depending on the decoupling approach employed. The first group [22, 23, 25, 26, 28, 30] utilizes the Zangger-Sterk approach [22], which achieves broadband homonuclear decoupling by combining a hard 180° and a selective 180° proton pulse, the latter applied under the action of a weak gradient field pulse to give an effect that is both spatially- and frequency-selective. As a result, in a given slice of the sample the on-resonance magnetization experiences no net effect, whereas all other proton magnetizations are inverted, refocusing any homonuclear scalar couplings to the observed spin. The second group [24, 27, 29, 31] of experiments performs broadband homonuclear decoupling with a bilinear rotation decoupling (BIRD) module [32], utilizing isotope selection instead of the slice/chemical shift filtering of the Zangger-Sterk approach. Depending on the phases

of BIRD pulse elements, either the direct or the remote protons attached to $^{13}C/^{15}N$ isotopes can be independently and selectively inverted.

The BIRD approach is used in the variants of the gradient enhanced CLIP/CLAP-HSQC experiments presented here, and yields spectra with simple, pure absorptive in- or anti-phase F_2 doublets displaying only the desired $^1J_{XH}$ splitting in isotropic or ($^1J_{XH}$ $+^1D_{XH}$) splitting in anisotropic solution, respectively and allowing high spectral resolution along the F_2 dimension. The one exception is that because the BIRD module does not distinguish between methylene protons, geminal ^1H-^1H couplings are not suppressed.

Broadband proton-decoupled CLIP- and CLAP HSQC experiments

In the modified CLIP/CLAP-HSQC experiments reported here, broadband proton decoupling in the ^1H dimension is achieved by replacing the conventional data acquisition of a free induction decay (FID) $s(t_2)$ at the end of the HSQC pulse sequence with a second evolution time, t_2, at the centre of which a hard 180° proton pulse and a BIRD pulse sequence element are applied in succession, followed by acquisition of a FID $s(t_3)$. The BIRD$^{(d)}$ pulse selectively inverts all proton magnetization directly attached to the X nuclei, but leaves the magnetizations of remotely bound protons and X nuclei unperturbed. In combination with the non-selective 180° proton pulse, therefore, the net effect is for the ^1H chemical shift and the heteronuclear one-bond coupling to continue to evolve throughout t_2. The measurement is repeated, acquiring FIDs $s(t_3)$ while incrementing t_2 in steps of 1/*sw2*, where the second indirect spectral width, *sw2*, is large compared to the widths of the proton multiplets. Once a full dataset $s(t_1, t_2, t_3)$ has been acquired, a pseudo-2D dataset is produced by stitching together chunks of $s(t_3)$ of duration 1/*sw2* for successive increments of t_2. The result is a pseudo-2D dataset $s(t_1, t'_2)$ in which signal evolves as normal (δ_C only) as a function of t_1, and as a pure shift ^1H signal in t'_2 (δ_H , $^2J_{HH}$ and $^1J_{CH}$ only). Typically *sw2* is 40 - 100 Hz, and 16 – 32 FIDs $s(t_3)$ are acquired, giving a maximum t'_2 of 160 – 800 ms and yielding ample spectral resolution for coupling constant measurement. It is important to note that the best results require very careful timing of the BIRD$^{(d)}$ and ^1H 180° pulse decoupling elements.

Therefore, the correct setting of the delays in the sequences of Fig. 1, as detailed in the figure legend, is critical.

As in the original CLIP-HSQC experiment [10], a carbon 90° pulse is employed to purge the undesired residual dispersive antiphase proton magnetization prior to detection. In the case of the CLAP-HSQC sequence, proton magnetization is detected in antiphase, so only a short spin-echo sequence to accommodate the coherence selection gradient pulse (G_4) follows, and the purging carbon pulse is omitted here.

The broadband proton-decoupled sequences of Fig. 1 have been tested on the small model compounds depicted in Scheme 1.

First, to investigate the robustness and tolerance of the experiments with regard to mismatch of the BIRD/INEPT delays in the sequence, a ^{13}C-labeled compound, [C-1]-methyl-α,β-D-glucopyranoside (**1**), was used. The results are shown in Fig. 2, which presents the C-1 doublets obtained with the broadband proton-decoupled CLAP-HSQC sequence using BIRD/INEPT delays adjusted to a range of nominal one-bond heteronuclear coupling constant spanning 100 to 180 Hz. It can clearly be seen that the intensities of the signals are, as expected, significantly degraded when the delays are mismatched to the coupling constant, but that the pure absorptive quality of the lineshapes remains basically unaffected, allowing accurate measurement of couplings even in anisotropic samples where net coupling constants vary widely. These results clearly demonstrate that the proposed sequences, used in combination with the pulsed field gradient coherence selection scheme illustrated in Fig. 1, efficiently remove the undesired residual dispersive coherences arising from the mismatch between delays and $^1J_{CH}$.

Applications of the broadband proton-decoupled CLIP/CLAP-HSQC experiments of Fig. 1 under isotropic and partially orienting sample conditions are demonstrated using model compound (**2**) (Scheme 1). A comparison between CLIP- and CLAP-HSQC spectra acquired with the conventional sequence [10] and the broadband decoupled sequence of Fig. 1 is given in Fig. 3. The selected carbon traces presented at the right hand side of the corresponding spectra nicely demonstrate that the decoupled experiments result in collapsed proton multiplets for XH spin systems. The pure absorptive in- or

antiphase doublets, with splittings due solely to the desired one-bond couplings, allow the direct and accurate determination of the scalar coupling constants.

To investigate their potential use for RDC measurement, we have also tested the performance of the new sequences on the same model compound (**2**) but this time dissolved in a weakly-orienting liquid crystalline phase of ether/alcohol mixture, as proposed by Rückert and Otting [11]. The high quality of the spectra and the selected carbon traces, with pure absorptive in- or antiphase doublets, shown in Fig. 4 demonstrates the good performance of these experiments, and promises the reliable measurement of RDCs, as exemplified for selected multiplets of C5.

It should be mentioned here that the undesired extra signals marked by asterisks (*) in Fig. 4, which arise from the weakly orienting phase in the anisotropic sample, show considerably reduced intensity in the broadband proton-decoupled spectra, but this is simply due to T_2 relaxation during the extended acquisition scheme of the decoupled sequences.

It is also important to note that following the IPAP-approach, as proposed earlier [16] (that is, adding and subtracting CLIP- and CLAP-HSQC spectra) allows quantitative extraction of one-bond coupling constants even in the case of complete overlap of α and β components of different doublets.

Broadband proton-decoupled, pure shift HSQC experiment

With a slight modification of the CLIP-HSQC sequence described above, a new method for generating broadband proton-decoupled (pure shift) HSQC (PS-HSQC) spectra is proposed. Such spectra have hitherto required a different experimental approach [24].

The PS-HSQC sequence depicted in Fig. 5 starts with the CLIP-HSQC block of the sequence in Fig. 1, but here the last purging carbon 90° pulse (which becomes superfluous when X-decoupling is used during detection) is omitted. In addition, the acquisition scheme detailed in the previous section is extended with two elements: 1) an appropriately-positioned carbon inversion 180° pulse (shown in grey) is needed to refocus the evolution of one-bond heteronuclear coupling between the detected FID chunks; and 2) composite pulse X-decoupling is turned on during FID acquisition $s(t_3)$ to

remove the undesired heteronuclear coupling interactions and so to obtain a fully decoupled, pure shift (PS) X-^{1}H correlation spectrum.

The beneficial features of the PS-HSQC sequence presented are illustrated in Fig. 6, which compares the HSQC spectra of D-sucrose and representative F_2 traces recorded with the standard non-decoupled and decoupled experiments. It is evident from the spectra presented that the removal of proton-proton splittings from X-^{1}H correlation spectra yields a considerable resolution improvement, making unambiguous spectral assignments and automated analyses feasible even in crowded spectra. The reduction of signal width due to proton-proton broadband decoupling, together with the pseudo-3D acquisition scheme employed, is particularly interesting for the collection of high resolution data. Specifically, in the PS-HSQC experiment presented, the resolution attainable in the direct dimension is not limited by the sample heating of X-decoupling during detection, but simply by the number of t_2 increments. Thus spectra with large numbers of t_2 increments, offering high resolution in F_2, can be collected even under the action of broadband heteronuclear decoupling.

An additional advantageous side-product of the BIRD$^{(d)}$ filter employed in the acquisition scheme presented is the efficient suppression of undesired long-range cross peaks arising from strong coupling effects, as demonstrated in Fig. 6. The strong coupling artifacts, marked by asterisk (*) in the standard HSQC spectrum (Fig. 6a) and the corresponding carbon traces at F4, F5, are almost entirely suppressed in the PS-HSQC spectrum (Fig. 6b), yielding a high quality pure shift correlation map for further spectral analysis. Note that this beneficial purging feature of the BIRD module has been utilized earlier in the standard HSQC experiment [33, 34].

To compare the sensitivity and robustness of the present pure shift HSQC experiment and the earlier method of Sakhaii et al. [24], HSQC spectra were recorded using the two pulse sequences with identical experimental parameters, but employing the same data acquisition scheme and processing, to ensure comparability. The signal intensities measured in the correlation spectra of Fig. 7 and illustrated by representative carbon traces at the right show that the sensitivity of the two experiments is comparable. Interestingly, the HSQC spectra recorded with intentionally mismatched INEPT/BIRD delays corresponding to $^{1}J_{XH}$ = 100 Hz show significant dissimilarity in the appearance of

artifacts. The purging and coherence selection gradient scheme employed in the broadband proton-decoupled HSQC sequence of Fig. 5 seem to suppress the effects of the proportion of magnetization that does not experience perfect rotation by the BIRD$^{(d)}$ module with high efficiency, yielding clean and artifact-free spectra even for a wide range of BIRD delays and hence for a wide range of one-bond coupling constants.

As noted earlier, the basic BIRD approach to broadband homonuclear decoupling is not able to suppress the effects of geminal couplings. Thus in Figs. 3, 4 and 7 the F_2 multiplets corresponding to CH_2 groups with non-equivalent (diastereotopic) geminal protons are doublets of doublets, with both $^1J_{CH}$ and $^2J_{HH}$ splittings. Example traces extracted at carbon C7 for compound **2** in Fig. 3 also illustrate this characteristic multiplet structure of CH_2 moieties. A method for the suppression of these undesired splittings will be the subject of a later publication.

In order to study the improvements in resolution that can be achieved for macromolecules, a ^{1}H-^{15}N HSQC experiment incorporating the proposed broadband proton decoupling scheme during acquisition was carried out on a ^{15}N-labeled, 55 amino acid residue, *Penicillium* antifungal protein (PAF) [35, 36]. As expected, decoupling of proton-proton interactions yields a significant decrease in F_2 linewidths (illustrated in Fig. 8), allowing direct and accurate measurements of NH chemical shifts and of cross peak intensities from the broadband decoupled singlets using automated peak picking.

4. *Conclusions and future outlook*

The broadband proton-decoupled CLIP/CLAP-HSQC experiments proposed here allow direct and accurate measurement of one-bond heteronuclear coupling constants and their dipolar contributions in XH moieties, and greatly simplified measurements in XH_2. The coupling constants can be determined directly, by measuring the splitting of pure absorptive in- or antiphase F_2 doublets, or by measuring the frequency difference between the relevant α and β multiplet components in the edited (added and subtracted) IPAP spectra. The latter approach allows the extraction of one-bond couplings even in the case of complete overlap of multiplet components. The robustness of the decoupled sequences presented with respect to variation in $^1J_{XH}$ ensures their applicability for RDC measurement, where wide distributions of $(^1J_{XH} + {}^1D_{XH})$ are common.

We acknowledge work going in a similar direction by the group of Luy. (T. Reinsperger, B. Luy, J. Magn. Reson. (submitted in parallel) [37]).

Modification of HSQC-based relaxation sequences, such as T_1, T_2, NOE, cross-correlated relaxation and relaxation dispersion experiments, to use the pure shift approach presented is in progress, with the promise of considerable benefits in the automated analysis of the resulting pure shift HSQC spectra.

Acknowledgements:

The authors thank Sára Balla for her skilful technical assistance in preparation of anisotropic samples. Dr. Gyula Batta and Dr. Mihály Herczeg are acknowledged for their generous gifts of ^{15}N-labeled PAF and the monosaccharide sample, respectively. Financial support from TÁMOP-4.2.2/A-11/1/KONV-2012-0025 and OTKA K 105459 (to K.E.K), from TÁMOP 4.2.4. A/2-11-1-2012-0001 (to I.T.), from Richter Gedeon Talentum Alapítvány (Ph.D. scholarship to I.T.), from ERC starting grant No 257041 (to C.M.T.), from the Merck Society for Arts and Science Foundation (Ph.D. scholarship to L.K.), from the Engineering and Physical Sciences Research Council (grant numbers EP/I007989 and EP/H024336) is gratefully acknowledged.

Scheme 1.

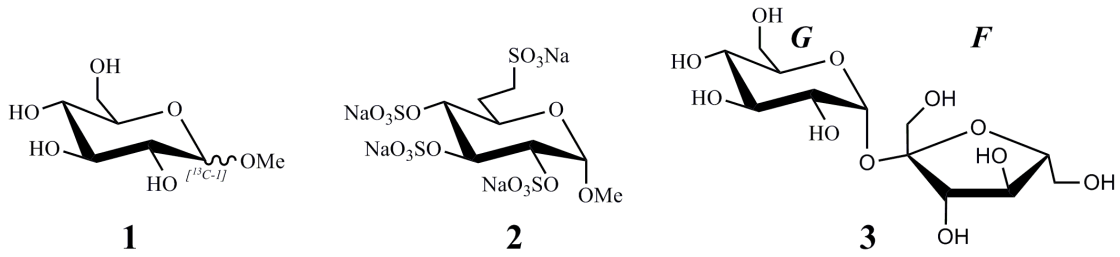

Figures and legends:

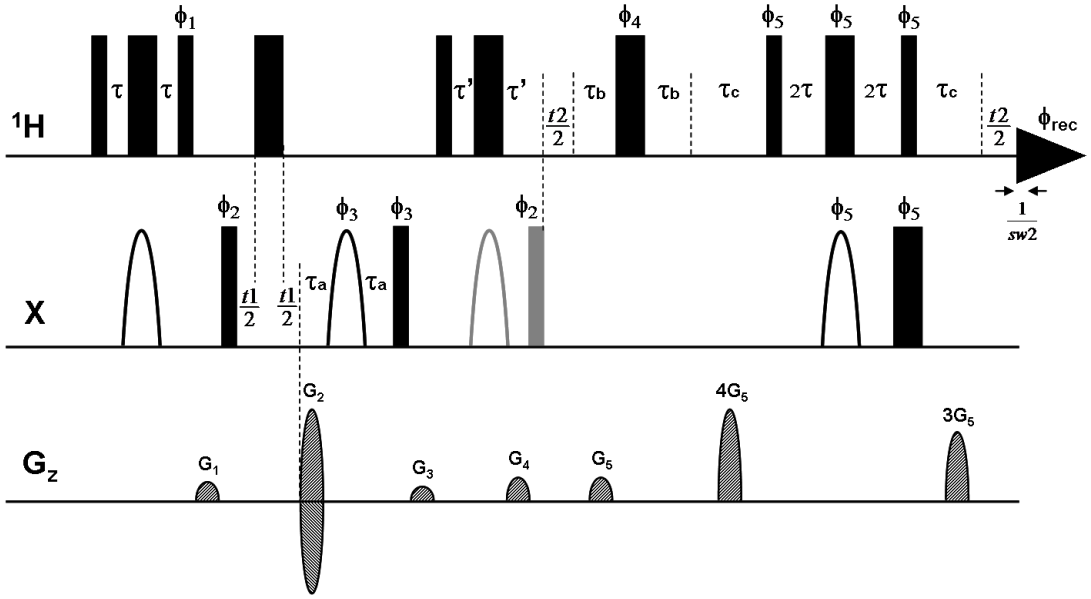

Fig. 1. Broadband proton-decoupled CLIP- and CLAP-HSQC experiments designed for the measurement of ($^1J_{CH}$ + $^1D_{CH}$) couplings. Narrow and wide filled bars correspond to 90° and 180° pulses, respectively, with phase *x* unless indicated otherwise. Smoothed chirp inversion and refocusing X pulses are shown as half-ellipses. Phases are ϕ_1 = *y*; ϕ_2 = *x*, *-x*; ϕ_3 = *x*, *x*, *-x*, *-x*; ϕ_4 = *y*, *y*, *y*, *y*, *y*, *y*, *y*, *y*, *-x*, *-x*, *-x*, *-x*, *-x*, *-x*, *-x*, *-x*; ϕ_5 = *y*, *y*, *y*, *y*, *-x*, *-x*, *-x*, *-x*; and ϕ_{rec} = *x*, *-x*, *-x*, *x*, *-x*, *x*, *x*, *-x*, *-x*, *x*, *x*, *-x*, *x*, *-x*, *-x*, *x*. Delays are set as follows: τ = 1/(4* $^1J_{XH}$), τ_a = p16 + d16, τ_b = 1/(4*sw2), τ_c = p16 + d16 + 350 μs, $\tau'_{(CLIP)}$ = τ; $\tau'_{(CLAP)}$ = p16 + d16. Coherence order selection and echo-antiecho phase sensitive detection in the X-dimension are achieved with gradient pulses G_2 and G_4 in the ratio 80 : 20.1 for ^{13}C and 80 : 8.1 for ^{15}N, respectively. Purging gradient pulses G_1, G_3 are set to 15 %, 11 % of maximum gradient strength (50 G/cm), typically of 1 ms duration (p16)

followed by a recovery delay d16 = 50 μs. Coherence selection gradient pulses used in the extra proton-decoupled dimension have G_5 = 18 %. In the CLIP-HSQC sequence an additional carbon 90° pulse (shown in grey) is employed to remove the undesired residual dispersive antiphase proton magnetization prior to detection, as proposed by Enthart et al. [10]. In contrast, in the CLAP-HSQC experiment the antiphase proton magnetization is retained and detected after X → ^{1}H back-transfer, so only a short spin-echo sequence (2*τ') with a proton 180° pulse in the middle is used to accommodate the gradient pulse G_4. The purging carbon 90° pulse and a carbon 180° pulse (shown in grey) used in the CLIP-experiment are omitted in this case.

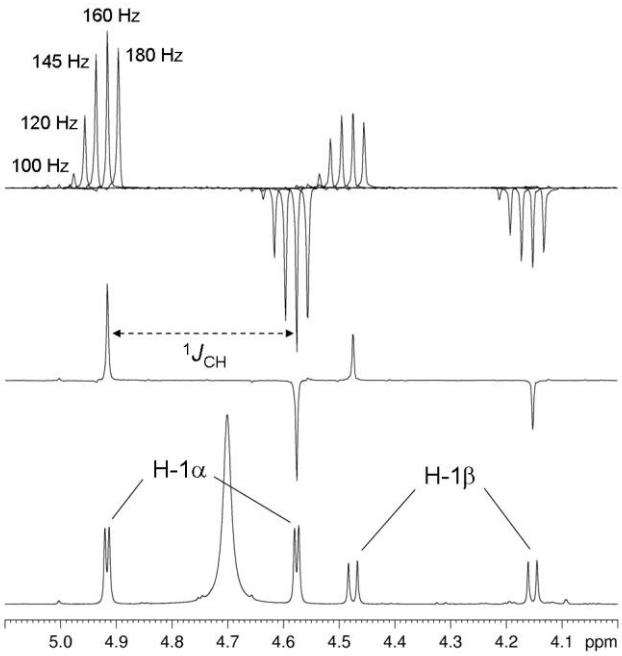

Fig. 2. Illustration of the robustness of the proposed CLAP-HSQC experiment with regard to mismatch between the INEPT and BIRD delays in the sequence and $^1J_{XH}$. Spectra of ^{13}C-labeled [C-1]-methyl-α,β-D-glucopyranoside were recorded using the sequence of Fig. 1 with the incremented delay t_1 replaced by a constant delay of 3 μs, to give pure shift 1D spectra. These were recorded with different durations of INEPT and BIRD delays (corresponding to the values of $^1J_{XH}$ shown), and were normalized to allow proper evaluation of the relative signal intensities and their dependence on the delays. Spectra were recorded with spectral widths in the ^{1}H dimension = 6.0371 ppm, relaxation

delay = 1.7 s, number of scans = 4, number of t_2 increments (i.e. number of FID chunks) = 32, duration of FID chunk = 21.197 ms, number of data points of constructed FID in ^{1}H dimension = 4096 complex data points.

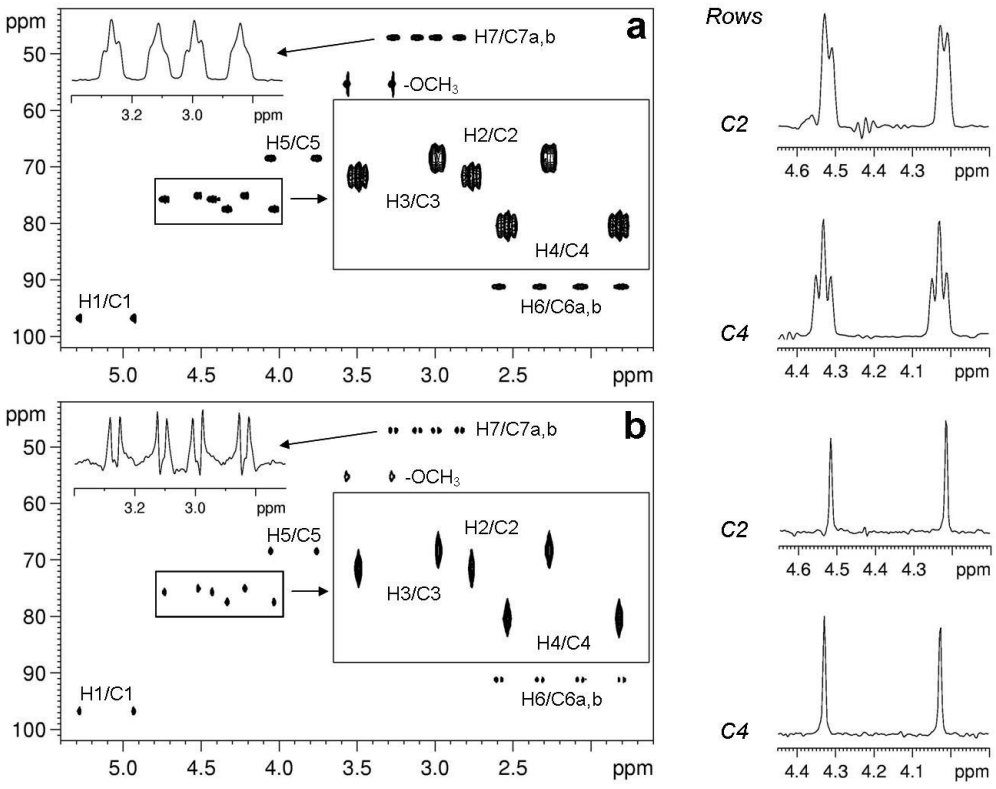

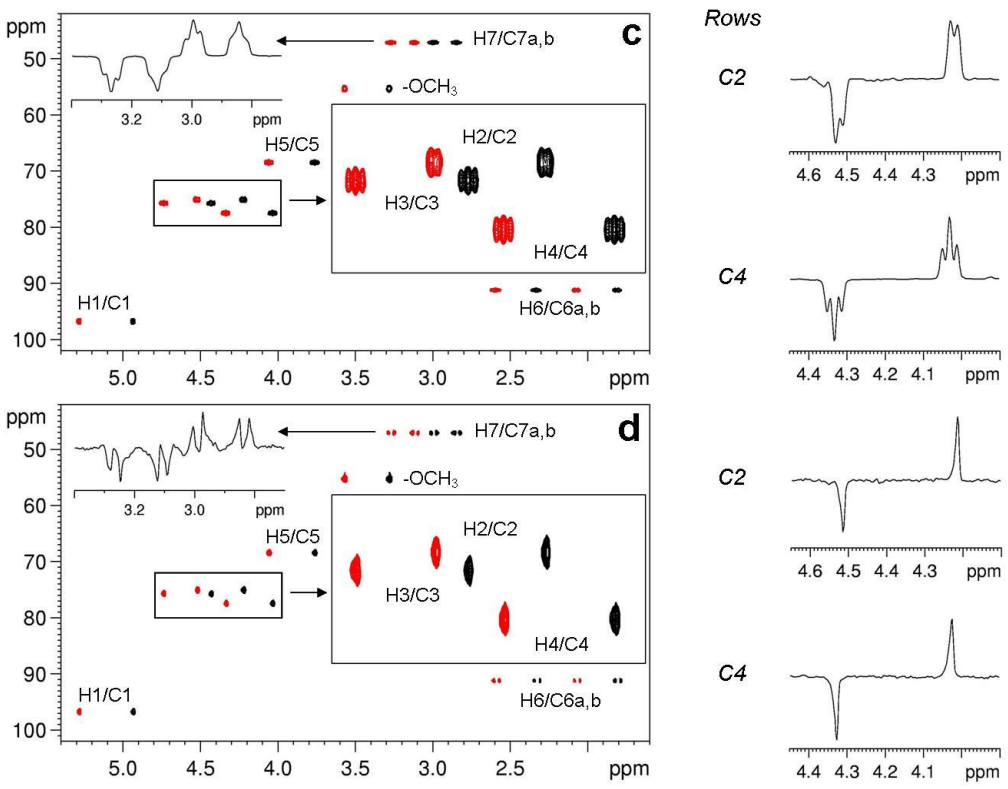

Fig. 3. Representative CLIP- and CLAP-HSQC spectra recorded with the conventional sequences [10] (a,c) and the new broadband proton-decoupled sequences of Fig. 1 (b,d) on an isotropic sample of compound **2** dissolved in D_2O. The carbon traces shown next to the corresponding spectra illustrate the characteristic differences in multiplet structure observed in the different experiments. Spectra were recorded at 300 K with spectral width in ^{13}C (^{1}H) dimension = 65.0 (4.9887) ppm, relaxation delay = 1.7 s, number of t_1 increments = 200, number of scans = 64 using the conventional CLIP/CLAP-HSQC sequences. The broadband decoupled spectra were collected with number of scans = 4, number of t_2 increments (i.e. number of FID chunks) = 16, duration of FID chunk = 20.842 ms, number of data points of constructed FID in ^{1}H dimension = 1664 complex data points.

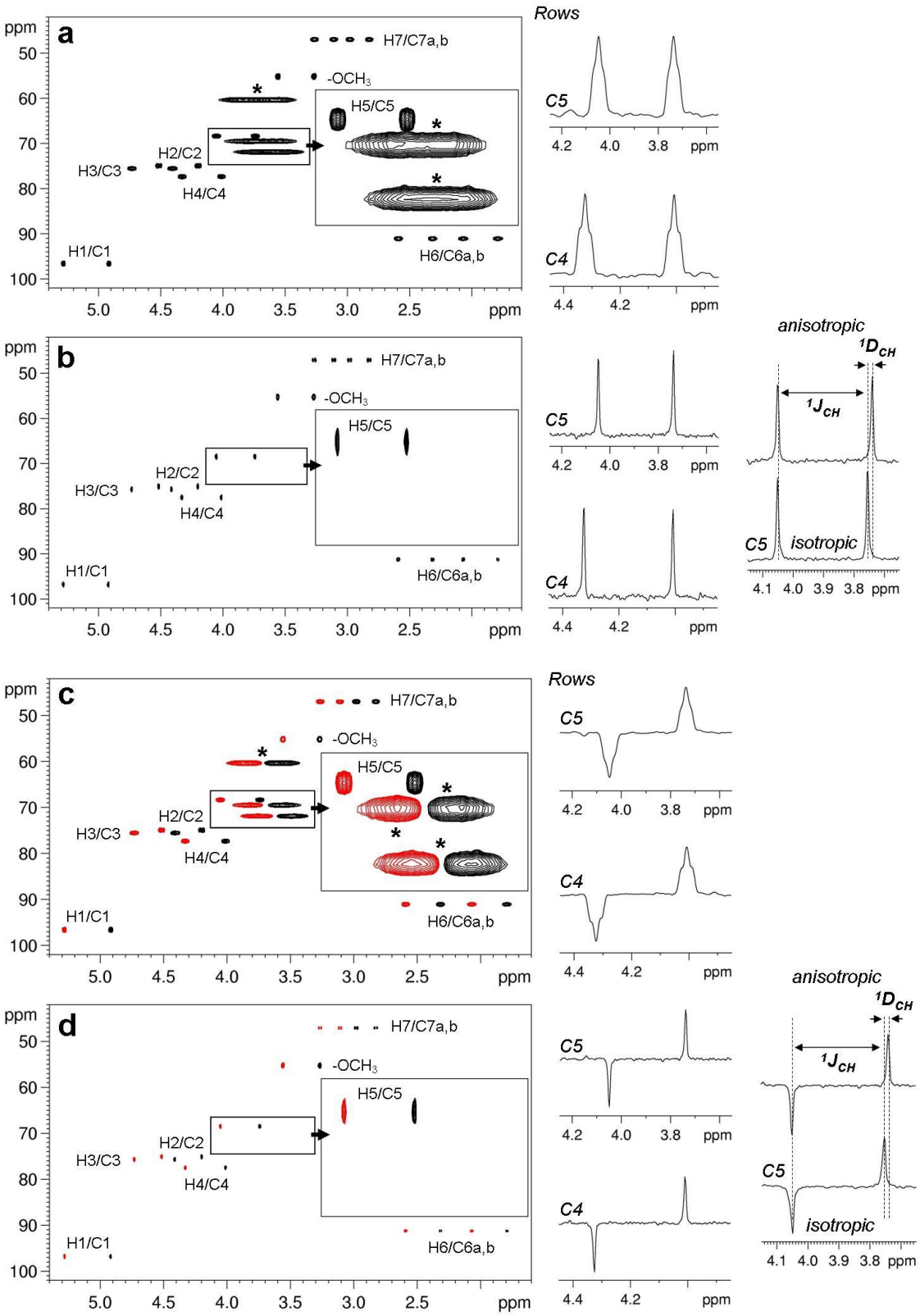

Fig. 4. Representative CLIP- and CLAP-HSQC spectra recorded with the conventional sequences [10] (a,c) and the broadband proton-decoupled sequences of Fig. 1 (b,d) on an

anisotropic sample of compound **2** dissolved in the weakly-orienting phase Otting media [11]. The high quality of the spectra and of the carbon traces extracted confirm that the good performance of the experiments is maintained under anisotropic condition, ensuring the accuracy of dipolar contributions measured from the splittings, as shown for representative multiplets of C5. (Note: we use the convention of total coupling constant ($^1J_{XH} + {}^1D_{XH}$) throughout the text.) Spectra were recorded at 300 K with spectral widths in ^{13}C (^1H) dimension = 65.0 (6.0371) ppm, relaxation delay = 1.7 s, number of t_1 increments = 200, number of scans = 64 using the conventional CLIP/CLAP-HSQC sequences. The broadband decoupled spectra were collected with number of scans = 8, number of t_2 increments (i.e. number of FID chunks) = 16, duration of FID chunk = 21.197 ms, number of data points of constructed FID in ^1H dimension = 2048 complex data points.

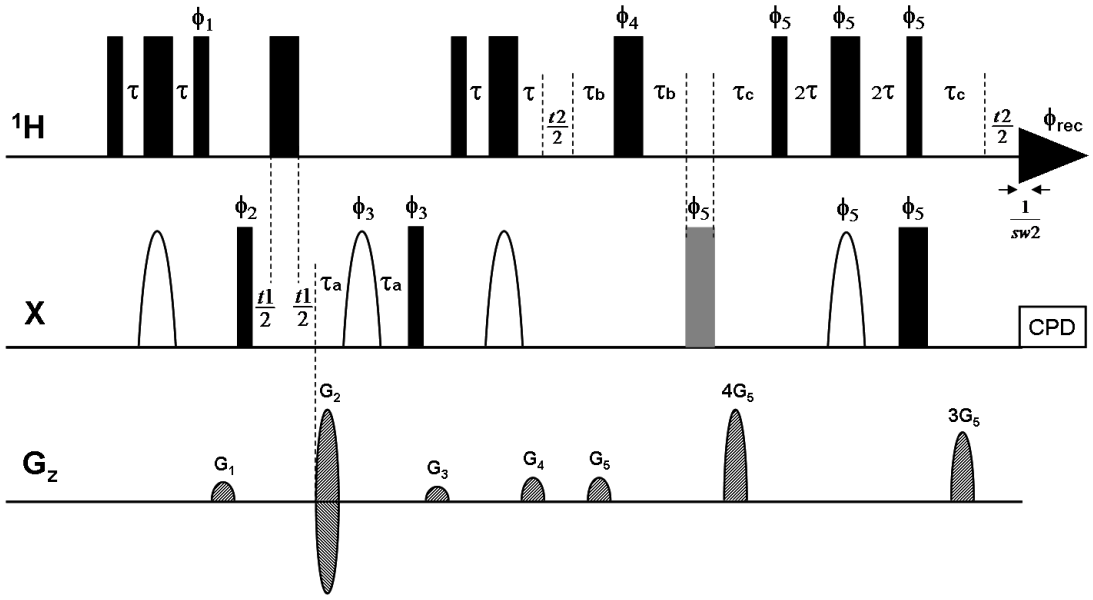

Fig. 5. Scheme of the broadband proton-decoupled (pure shift) HSQC (PS-HSQC) experiment. Narrow and wide filled bars correspond to 90° and 180° pulses, respectively, with phase *x* unless indicated otherwise. Smoothed chirp inversion and refocusing X pulses are shown as half-ellipses. Phases are $\phi_1 = y$; $\phi_2 = x, -x$; $\phi_3 = x, x, -x, -x$; $\phi_4 = y, y, y, y, y, y, y, y, -x, -x, -x, -x, -x, -x, -x, -x$; $\phi_5 = y, y, y, y, -x, -x, -x, -x$; and $\phi_{rec} = x, -x, -x, x, -x, x, x, -x, -x, x, x, -x, x, -x, -x, x$. Delays are set as follows: $\tau = 1/(4* {}^1J_{XH})$, τ_a = p16 + d16, $\tau_b = 1/(4*sw2)$, τ_c = p16 + d16 + 350 μs. Coherence order selection and echo-antiecho

phase sensitive detection in the X-dimension are achieved with gradient pulses G_2 and G_4 in the ratio 80 : 20.1 for ^{13}C and 80 : 8.1 for ^{15}N, respectively. Purging gradient pulses G_1, G_3 are set to 15 %, 11 % of maximum gradient strength (50 G/cm), typically with 1 ms duration (p16) followed by a recovery delay d16 = 50 μs. Coherence selection gradient pulses are used in the extra proton-decoupled dimension with G_5 = 18 %. An additional carbon 180° pulse (shown in grey) is employed to refocus the evolution of one-bond heteronuclear coupling between FID chunks. CPD decoupling is turned on during detection.

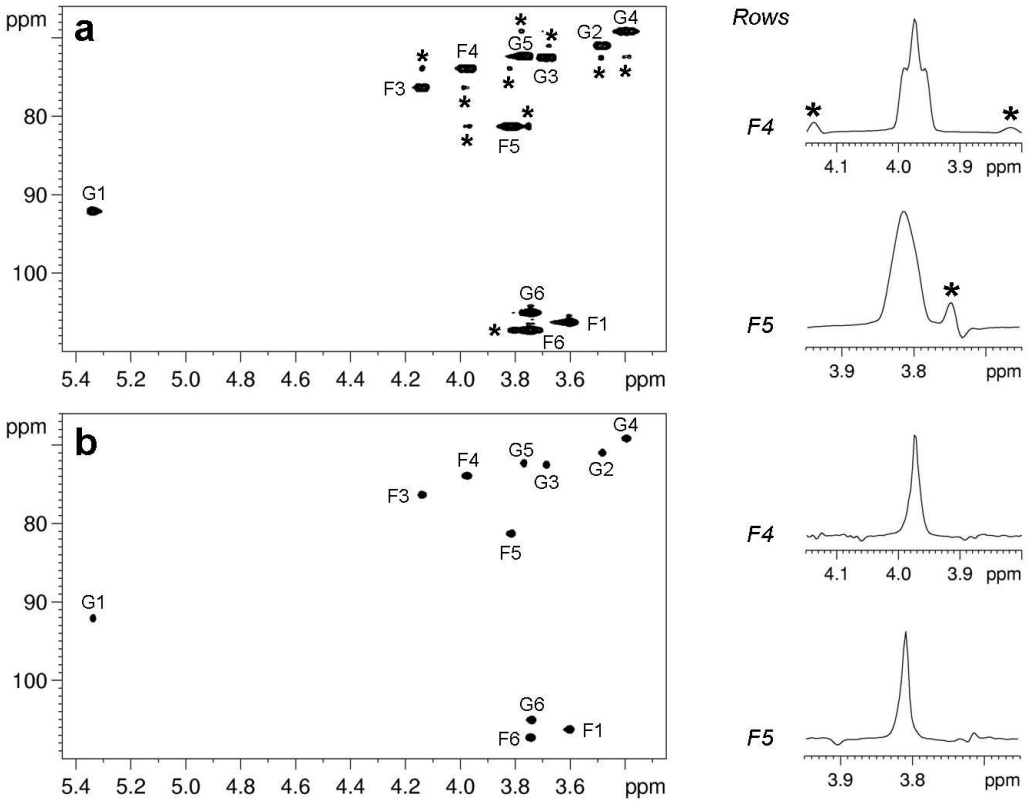

Fig. 6. Comparison of HSQC spectra recorded without (a) and with (b) broadband proton decoupling for D-sucrose dissolved in D_2O (30 mg/500 μl). Long-range correlation artifacts resulting from strong coupling effects observed in spectrum (a) acquired with the standard gradient enhanced HSQC sequence are labeled with asterisks (*) in both the correlation map and the selected carbon traces. In the broadband decoupled spectrum (b) these artifacts are almost entirely suppressed, resulting in a high quality pure shift correlation map with collapsed proton multiplet structure, suitable for automated spectral

analysis. Spectra were recorded with spectral widths in ^{13}C (^{1}H) dimension = 45.0 (6.0371) ppm, relaxation delay = 1.7 s, number of t_1 increments = 180. Number of scans = 32 was used with the conventional HSQC sequence. The broadband decoupled spectrum was collected with number of scans = 2, number of t_2 increments (i.e. number of FID chunks) = 16, duration of FID chunk = 21.197 ms, number of data points of constructed FID in ^{1}H dimension = 2048 complex data points.

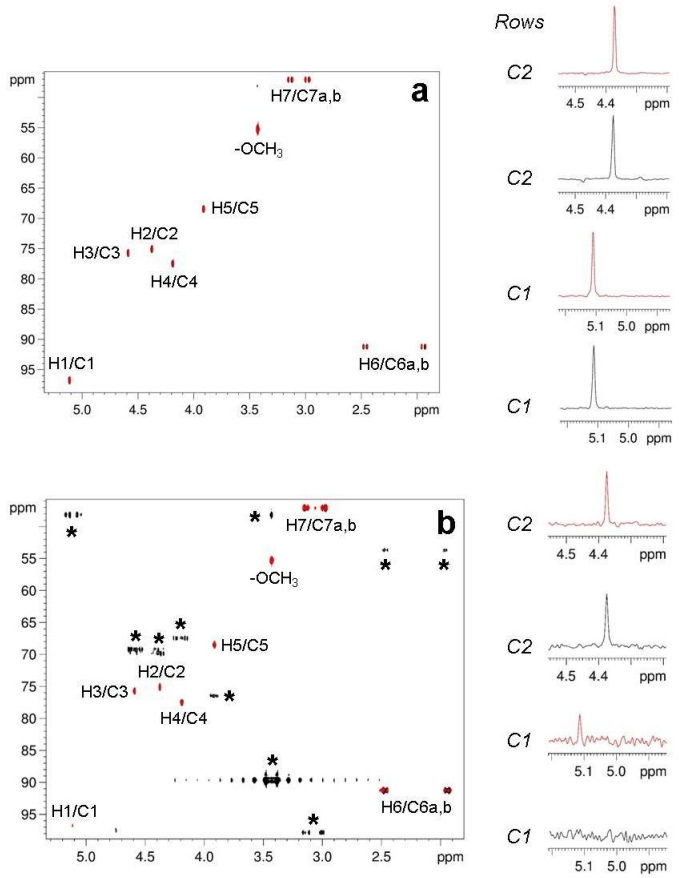

Fig. 7. Comparison of HSQC spectra recorded with the present (red lines) and earlier reported [24] (black lines) broadband proton-decoupled sequences for an isotropic sample of compound **2**. Experiments were performed with the same experimental parameters and data acquisition scheme, and the same data processing was used. To compare the sensitivity and robustness of sequences, spectra were collected with INEPT/BIRD delays adjusted to nominal $^{1}J_{XH}$ values of 145 Hz (a) and 100 Hz (b) (deliberately misset), respectively. The intensities of the signals in the spectra displayed are normalized, allowing proper comparison of sensitivity and of artifact (marked by *) amplitudes.

Spectra were recorded with spectral widths in ^{13}C (^{1}H) dimension = 65.0 (4.9887) ppm, relaxation delay = 1.7 s, number of t_1 increments = 200, number of scans = 2, number of t_2 increments (i.e. number of FID chunks) = 16, duration of FID chunk = 20.842 ms, number of data points of constructed FID in ^{1}H dimension = 1664 complex data points.

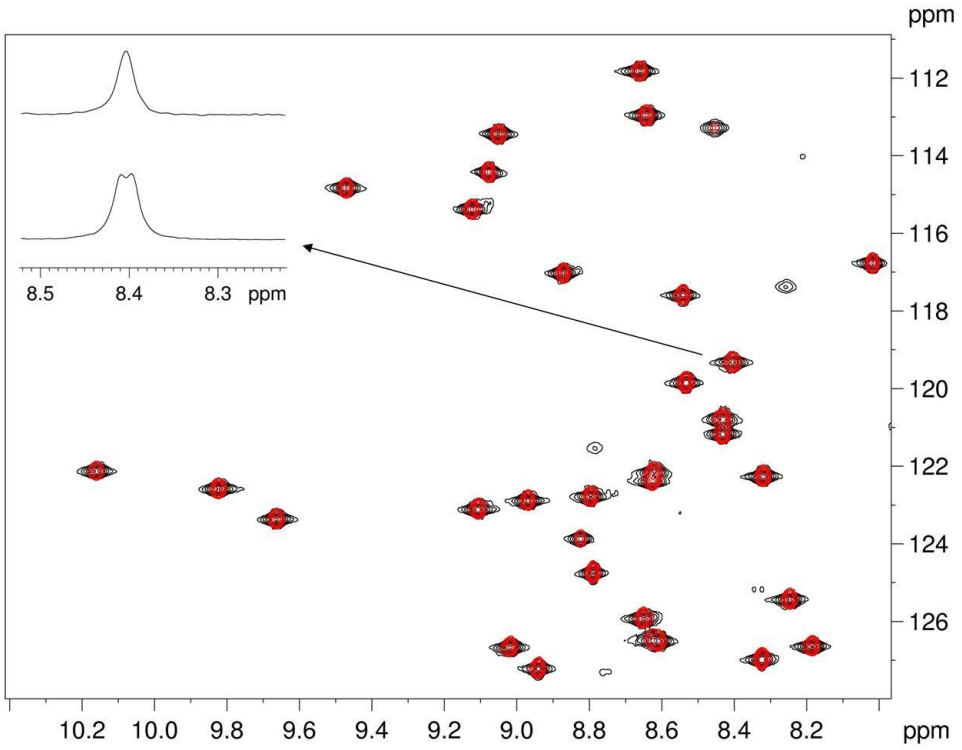

Fig. 8. Comparison of ^{1}H-^{15}N HSQC peak linewidths of PAF in spectra recorded without (black lines and lower trace at the left) and with (red lines and upper trace at the left) broadband proton decoupling. The advantage of the broadband decoupled sequence of Fig. 5 for macromolecules is demonstrated by the collapsed proton doublet structures, resulting in considerable reduction of the observed linewidth, and unequivocal peak definition for automated data analysis. Spectra were recorded with spectral widths in ^{15}N (^{1}H) dimension = 19.0 (4.9887) ppm, relaxation delay = 1.7 s, number of t_1 increments = 128. Number of scans = 64 was used with the conventional HSQC sequence. The broadband decoupled spectrum was collected with number of scans = 4, number of t_2 increments (i.e. number of FID chunks) = 16, duration of FID chunk = 21.245 ms, number of data points of constructed FID in ^{1}H dimension = 1696 complex data points.

References:

[1] E. de Alba, N. Tjandra, NMR dipolar couplings for the structure determination of biopolymers in solution, Prog. Nucl. Magn. Reson. Spectrosc., 40 (2002) 175-197.
[2] A. Bax, Weak alignment offers new NMR opportunities to study protein structure and dynamics, Protein Sci., 12 (2003) 1-16.
[3] J.H. Prestegard, C.M. Bougault, A.I. Kishore, Residual Dipolar Couplings in Structure Determination of Biomolecules, Chem. Rev., 104 (2004) 3519-3540.
[4] M. Blackledge, Recent progress in the study of biomolecular structure and dynamics in solution from residual dipolar couplings, Prog. Nucl. Magn. Reson. Spectrosc., 46 (2005) 23-61.
[5] J.R. Tolman, K. Ruan, NMR residual dipolar couplings as probes of biomolecular dynamics, Chem. Rev., 106 (2006) 1720-1736.
[6] C.M. Thiele, Residual Dipolar Couplings (RDCs) in Organic Structure Determination, Eur. J. Org. Chem., 2008 (2008) 5673-5685.
[7] G. Kummerlöwe, B. Luy, Chapter 4 - Residual Dipolar Couplings for the Configurational and Conformational Analysis of Organic Molecules, in: Annual Reports on NMR Spectroscopy, Academic Press, 2009, pp. 193-232.
[8] B. Böttcher, C.M. Thiele, Determining the Stereochemistry of Molecules from Residual Dipolar Couplings (RDCs), eMagRes DOI: 10.1002/9780470034590.emrstm1194.
[9] B. Böttcher, V. Schmidts, J.A. Raskatov, C.M. Thiele, Determination of the Conformation of the Key Intermediate in an Enantioselective Palladium-Catalyzed Allylic Substitution from Residual Dipolar Couplings, Angew. Chem. Int. Ed., 49 (2010) 205-209.
[10] A. Enthart, J.C. Freudenberger, J. Furrer, H. Kessler, B. Luy, The CLIP/CLAP-HSQC: Pure absorptive spectra for the measurement of one-bond couplings, J. Magn. Reson., 192 (2008) 314-322.
[11] M. Rückert, G. Otting, Alignment of Biological Macromolecules in Novel Nonionic Liquid Crystalline Media for NMR Experiments, J. Am. Chem. Soc., 122 (2000) 7793-7797.
[12] C. Griesinger, O.W. Sørensen, R.R. Ernst, Practical aspects of the E.COSY technique. Measurement of scalar spin-spin coupling constants in peptides, J. Magn. Reson., 75 (1987) 474-492.
[13] P. Andersson, A. Annila, G. Otting, An α/β-HSQC-α/β Experiment for Spin-State Selective Editing of IS Cross Peaks, J. Magn. Reson., 133 (1998) 364-367.
[14] P. Andersson, J. Weigelt, G. Otting, Spin-state selection filters for the measurement of heteronuclear one-bond coupling constants, J. Biomol. NMR, 12 (1998) 435-441.
[15] F. Cordier, A.J. Dingley, S. Grzesiek, A doublet-separated sensitivity-enhanced HSQC for the determination of scalar and dipolar one-bond J-couplings, J. Biomol. NMR, 13 (1999) 175-180.
[16] M. Ottiger, F. Delaglio, A. Bax, Measurement of *J* and Dipolar Couplings from Simplified Two-Dimensional NMR Spectra, J. Magn. Reson., 131 (1998) 373-378.
[17] K. Pervushin, R. Riek, G. Wider, K. Wüthrich, Attenuated T_2 relaxation by mutual cancellation of dipole-dipole coupling and chemical shift anisotropy indicates an avenue

to NMR structures of very large biological macromolecules in solution, Proc. Natl. Acad. Sci. U. S. A., 94 (1997) 12366-12371.
[18] M. Czisch, R. Boelens, Sensitivity Enhancement in the TROSY Experiment, J. Magn. Reson., 134 (1998) 158-160.
[19] J. Weigelt, Single Scan, Sensitivity- and Gradient-Enhanced TROSY for Multidimensional NMR Experiments, J. Am. Chem. Soc., 120 (1998) 10778-10779.
[20] K. Fehér, S. Berger, K.E. Kövér, Accurate determination of small one-bond heteronuclear residual dipolar couplings by F1 coupled HSQC modified with a G-BIRD$^{(r)}$ module, J. Magn. Reson., 163 (2003) 340-346.
[21] C.M. Thiele, W. Bermel, Speeding up the measurement of one-bond scalar (^1J) and residual dipolar couplings (^1D) by using non-uniform sampling (NUS), J. Magn. Reson., 216 (2012) 134-143.
[22] K. Zangger, H. Sterk, Homonuclear broadband-decoupled NMR spectra, J. Magn. Reson., 124 (1997) 486-489.
[23] M. Nilsson, G.A. Morris, Pure shift proton DOSY: diffusion-ordered 1H spectra without multiplet structure, Chem. Commun., (2007) 933-935.
[24] P. Sakhaii, B. Haase, W. Bermel, Experimental access to HSQC spectra decoupled in all frequency dimensions, J. Magn. Reson., 199 (2009) 192-198.
[25] J.A. Aguilar, S. Faulkner, M. Nilsson, G.A. Morris, Pure Shift 1H NMR: A Resolution of the Resolution Problem?, Angew. Chem. Int. Ed., 49 (2010) 3901-3903.
[26] G.A. Morris, J.A. Aguilar, R. Evans, S. Haiber, M. Nilsson, True Chemical Shift Correlation Maps: A TOCSY Experiment with Pure Shifts in Both Dimensions, J. Am. Chem. Soc., 132 (2010) 12770-12772.
[27] J.A. Aguilar, M. Nilsson, G.A. Morris, Simple Proton Spectra from Complex Spin Systems: Pure Shift NMR Spectroscopy Using BIRD, Angew. Chem. Int. Ed., 50 (2011) 9716-9717.
[28] J.A. Aguilar, A.A. Colbourne, J. Cassani, M. Nilsson, G.A. Morris, Decoupling Two-Dimensional NMR Spectroscopy in Both Dimensions: Pure Shift NOESY and COSY, Angew. Chem. Int. Ed., 51 (2012) 6460-6463.
[29] A. Lupulescu, G.L. Olsen, L. Frydman, Toward single-shot pure-shift solution 1H NMR by trains of BIRD-based homonuclear decoupling, J. Magn. Reson., 218 (2012) 141-146.
[30] N.H. Meyer, K. Zangger, Simplifying Proton NMR Spectra by Instant Homonuclear Broadband Decoupling, Angew. Chem. Int. Ed., 52 (2013) 7143-7146.
[31] L. Paudel, R.W. Adams, P. Király, J.A. Aguilar, M. Foroozandeh, M.J. Cliff, M. Nilsson, P. Sándor, J.P. Waltho, G.A. Morris, Simultaneously Enhancing Spectral Resolution and Sensitivity in Heteronuclear Correlation NMR Spectroscopy, Angew. Chem. Int. Ed., (2013) DOI: 10.1002/anie.201305709.
[32] J.R. Garbow, D.P. Weitekamp, A. Pines, Bilinear rotation decoupling of homonuclear scalar interactions, Chem. Phys. Lett., 93 (1982) 504-509.
[33] V. Rutar, T.C. Wong, W. Guo, Manipulated heteronuclear two-dimensional NMR bilinear pulses in the presence of strong coupling, J. Magn. Reson., 64 (1985) 8-19.
[34] G.V.T. Swapna, R. Ramachandran, N. Reddy, A.C. Kunwar, Virtual coupling effects in heteronuclear chemical-shift correlation spectroscopy, J. Magn. Reson., 88 (1990) 135-140.

[35] G. Batta, T. Barna, Z. Gáspári, S. Sándor, K.E. Kövér, U. Binder, B. Sarg, L. Kaiserer, A.K. Chhillar, A. Eigentler, É. Leiter, N. Hegedüs, I. Pócsi, H. Lindner, F. Marx, Functional aspects of the solution structure and dynamics of PAF – a highly-stable antifungal protein from Penicillium chrysogenum, FEBS J., 276 (2009) 2875-2890.
[36] G. Váradi, G.K. Tóth, Z. Kele, L. Galgóczy, Á. Fizil, G. Batta, Synthesis of PAF, an Antifungal Protein from P. chrysogenum, by Native Chemical Ligation: Native Disulfide Pattern and Fold Obtained upon Oxidative Refolding, Chemistry – A European Journal, 19 (2013) 12684-12692.
[37] T. Reinsperger, B. Luy, Homonuclear BIRD-Decoupled Spectra for Measuring One-Bond Couplings with Highest Resolution: CLIP/CLAP-RESET and Constant-Time-CLIP/CLAP-RESET, J. Magn. Reson., (2013) submitted.